Scientific paper

Development of Silicate-Based Surface Impregnation Solution with High Permeability for Restoration of Degraded Concrete

Tatsuya Kitada[1,2] and Zhuguo Li[3*]

Abstract

In this study, for developing a silicate-based surface impregnation solution with high permeability to repair degraded concrete from the surface to the interior, experiments were conducted to investigate the effect of blending sodium hydroxide (NaOH) on the permeability of the lithium silicate solution (LS) that is one of generally used silicate surface impregnation materials. The high permeability of the modified LS solution, composed of LS, NaO, and water, was confirmed by solution immersion test using several grades of concrete and heated concrete with different strengths, and by ICP-AES analysis. Appropriate NaOH blend significantly increased the penetration of LS into concrete. The appropriate NaOH blends and the mechanisms of increasing permeability were investigated by the setting time test of fresh pastes of modified LS solution and unheated or 650°C-heated Portland cement paste powders, and the SEM-EDS, XRD, TG-DTA analyses of hardened pastes. As a result, when NaOH is blended in an amount such that the Na/Si molar ratio of NaOH-modified LS solutions is in the range of 0.5-1.25, they have high permeability. The addition of NaOH reduces the solubility of $Ca(OH)_2$, being a hydrate of Portland cement (PC), and therefore delays the calcium silicate formation between $Ca(OH)_2$ and LS. This delay prevents the penetration path of LS from being quickly blocked by calcium silicate, thus LS permeability is improved. However, the addition of excessive NaOH destroys other hydrates of PC to dissolve Ca ions, instead increasing the calcium silicate formation. In addition, the blend of NaOH would increase the alkalinity of neutralized concretes.

1. Introduction

In recent years, for reducing the environmental burden of concrete structures, the importance of structural maintenance has been rising, and research on repair and reinforcement has gained attention in extending the service life of concrete structures. Major deterioration factors of concrete include neutralization, salt damage, alkali-silica reaction, and freeze-thaw action, etc. The penetration of aggressive substances such as moisture, chloride ions, oxygen, and carbon dioxide from the external environment causes the physical or/and chemical degradation of concrete. For example, neutralization occurs when atmospheric carbon dioxide infiltrates into concrete, initiating carbonation reaction and potentially causing corrosion of internal steel reinforcement. Steel bars whose passive film has been destroyed may rust in the presence of oxygen and water. Additionally, high temperatures during a fire causes degradation of concrete due to the decomposition of cement hydration products and the difference in the degree of thermal expansion of aggregates and hardened matrix cement paste, exhibiting strength reduction, neutralization, and cracks (Daungwilailuk et al. 2019; Joakim 2015).

The inhibition of water ingress from the surface of concrete structures has been shown to significantly improve the issues related to the deterioration (Ishibashi *et al.* 2002; Maehara and Iyoda 2018). In the pursuit of methods for inhibiting deterioration and preventive maintenance of concrete structures, surface impregnation has proved to be effective (Takeda *et al.* 2021). Surface impregnation is the application of impregnation agent on the surface of concrete structure. In Japan, the "Recommendation for Concrete Repair and Surface Protection of Concrete Structures" (JSCE 2005) was established for surface impregnation by the Japan Society of Civil Engineers. Surface impregnation agents can be broadly categorized into silane-based and silicate-based materials according to their primary components. Silane-based impregnation agents typically consist of alkylalkoxysilane monomers or oligomers, or a mixture thereof, forming a hydrophobic layer within a few millimeters on the concrete surface. The reported effects include preventing the penetration of moisture and chloride ions, as well as suppressing alkali-aggregate reactions (Hayashi *et al.* 2019). Unlike organic impregnation agents, silicate-based impregnation agents require fewer construction steps, are cost-effective, and preserve the appearance of concrete surfaces and facilitates easy inspection and maintenance because they are colorless and transparent solutions.

Silicate-based impregnation agents involve the penetration of sodium silicate or lithium silicate into concrete

[1]Engineer, Repair Technology Development Section, Dept. of Technology Development, Technology Headquarters, Kyokuto Kowa Corporation, Hiroshima, Japan.
[2]Graduate student, Graduate School of Sciences and Technology for Innovation, Yamaguchi University, Japan.
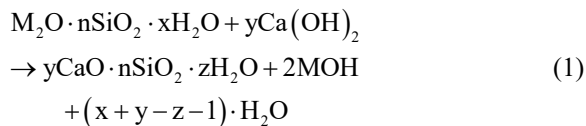[3]Professor, Graduate School of Sciences and Technology for Innovation, Yamaguchi University, Japan.
*Corresponding author, *E-mail*: li@yamaguchi-u.ac.jp

Table 1 NH-modified lithium silicate impregnations.

Series	Component (wt.%)			Chemical and physical features		
	Lithium silicate	10M Sodium hydroxide	Deionized water	Na/Si molar ratio	Solid content (%)	Specific gravity
Series 0.00 (LS only)	41.98	-	58.02	0.00	9.66	1.084
Series 0.25	41.98	1.40	56.62	0.25	11.05	1.098
Series 0.50	41.98	2.79	55.23	0.50	12.45	1.113
Series 0.75	41.98	4.19	53.83	0.75	13.85	1.129
Series 1.00	41.98	5.59	52.43	1.00	15.24	1.146
Series 1.25	41.98	6.99	51.03	1.25	16.64	1.163
Series 1.75	41.98	9.78	48.24	1.75	19.44	1.202
NH only Series	-	6.99	93.01	-	6.99	1.075
Series 1.25-30	75.68	12.59	11.73	1.25	30.00	1.413

for enhancing concrete properties. The basic reaction of silicate-based surface impregnations ($M_2O \cdot SiO_2 \cdot xH_2O$, M is monovalent alkali metal such as Na^+, K^+, Li^+) with $Ca(OH)_2$ in concrete is as Eq. (1).

$$M_2O \cdot nSiO_2 \cdot xH_2O + yCa(OH)_2$$
$$\rightarrow yCaO \cdot nSiO_2 \cdot zH_2O + 2MOH \quad (1)$$
$$+ (x + y - z - 1) \cdot H_2O$$

Calcium silicate, the product of the above reaction, fills the pores and cracks of the concrete and densifies the concrete, which increases the resistance of the concrete to the penetration of the aggressive substances, thus improving the durability of the concrete (Kurokawa and Miyazato 2015; Midorikawa *et al.* 2011). However, since the above reaction requires $Ca(OH)_2$, the modification effect is limited for the carbonated concrete, and this reaction reduces the carbonation resistance of the uncarbonated concrete (Kondo *et al.* 2019).

Silicate-based surface impregnation materials can only penetrate a few millimeters into concrete. Thus, the impregnation solution remains at the concrete surface, and cannot modify inside concrete (Someya and Kato 2014; Baltazar *et al.* 2014). This is because the product of the above reaction densifies the surface layer of concrete, thereby hindering the further spread of the impregnation material. Therefore, the silicate-based surface impregnation materials generally have a limited modifying effect on the surface layer of concrete and are primarily used to enhance durability of concrete rather than strength (Tran *et al.* 2018; Baltazar *et al.* 2014).

The authors found accidentally that the permeability of lithium silicate solution, one of the main conventional silicate-based surface impregnation materials, can be greatly improved by adding sodium hydroxide (NaOH) solution, compared to the lithium silicate solution alone. If the addition of NaOH solution can indeed increase the permeability of lithium silicate solution, not only the internal modification of concrete is available, but also neutralized concrete can be re-alkalized, known as chemical re-alkalization treatment of concrete that restores the alkalinity of concrete and improves the corrosive environment of steel by introducing alkaline components (alkali ions: positive

ions) into the concrete (Réus and Medeiros 2020).

For developing a silicate-based surface impregnation material with high permeability for restoring concretes damaged by aggressive substances or fire, in this study the authors investigated in detail the effect of NaOH addition on the permeability of lithium silicate solution in both normal concrete and heated concrete, and then discussed suitable blending ratio of NaOH. We also discussed the mechanism, by which the inclusion of NaOH increases the permeability of lithium silicate solution, through a combination of TG-DTA and XRD analyses, as well as setting time tests, using the hardened mixtures or fresh mixtures that were prepared by mixing the powders of hardened cement paste or 650°C-heated hardened cement paste and the lithium silicate solutions containing varying amounts of NaOH.

2. Permeability of NH-modified silicate impregnation

2.1 Components of NH-modified impregnations

Silicates commonly used as silicate-based surface impregnation materials include lithium silicate, sodium silicate, and potassium silicate. However, the former is less viscous compared to the latter two, so it is relatively easy to penetrate into concrete. Therefore, in this study, lithium silicate (LS) and sodium hydroxide solution (NH) were chosen to prepare NH-modified impregnations, as shown in **Table 1**. The specifications of used lithium silicate are shown in **Table 2**. The reference NH-modified impregnation was Series 1.25 with Na/Si molar ratio of 1.25, which was prepared by the lithium silicate, 10 mol/L NaOH, and deionized water in a ratio of 2:1:2 by volume.

Based on the mix proportions of Series 1.25 and keeping the dosage of lithium silicate constant, six solutions with different Na/Si molar ratios ranging from 0.25 to 1.75 were prepared by adjusting the amounts of NaOH solution and water. Additionally, referring to Series 1.25, we prepared a solution, marked as Series 1.25-30, to investigate the effect of solid concentration on permeability. This solution was prepared by increasing the amount of lithium silicate to achieve a high solid concentration of 30%.

Table 2 Specifications of aqueous lithium silica solution used.

Formula	Li$_2$O·nSiO$_2$ (n=3.6)
Chemical and physical features	SiO$_2$: 21% Li$_2$O : 2.9% pH (25°C): 10.0 to 11.4 Specific gravity (25°C): 1.18 to 1.22 Viscosity (25°C): 15 mPa·s or less

Table 3 Mix proportions and strength of the used concretes.

Notation	Water-cement ratio (W/C, %)	Unit mass (kg/m^3)							Compressive strength Fc (N/mm^2)
		W	C	S-1	S-2	G-1	G-2	WR	
G20	68	164	241	276	643	1000	-	2.7	24.4
G40	53	164	309	265	618	-	919	4.08	42.7
G60	37	168	454	221	516	937	-	5.45	60.0

Table 4 Raw materials of the used concretes.

Notation	Raw material	Fineness or grading	Density in surface dry state (g/cm^3)	Fineness modulus (F.M.) or solids content (S.C.)
C	Ordinary Portland cement	3500 cm^2/g (Blaine value)	3.15	-
S-1	Crushed sand	0-5 mm	2.58	2.9 (F.M.)
S-2	Sea sand	0-2 mm	2.73	2.9 (F.M.)
G-1	Crushed stone	5-20 mm	2.81	60.6% (S.C.)
G-2	Crushed stone	5-20 mm	2.57	59.2% (S.C.)
WR	Air entraining water reducing agent			

2.2 Concrete specimens

Concrete specimens of three strength grades were prepared to investigate the influence of concrete strength on the permeability of lithium silicate impregnation. Their mix proportions and compressive strengths are shown in **Table 3**, which had different water-to-cement ratios: 68% for G20, 53% for G40, and 37% for G60. And the raw materials used in the concretes are shown in **Table 4**. According to the standards of the Architectural Institute of Japan, G20, G40 and G60 can be regarded as normal concrete (compressive strength F$_c$<36 MPa), high-strength concrete (F$_c$≥36 MPa) and ultra-high-strength concrete (F$_c$≥60 MPa), respectively. The concrete specimens used for the compressive strength test were 100 mm diameter cylinders of height 100 mm, but either the prismatic specimens (100×100×400 mm) or the cylinders were used in the permeability experiment. After the specimens were cast, they were left to be cured in the air at 20±3°C for one day before demolding. Subsequently, they were immersed in a water tank at 20°C for water-curing until

they reached 28-day age, and then stored in a room at 20±3°C, R.H. 60±5% for about 28 days before immersing in the lithium silicate impregnations.

Two types of concrete specimens were used to investigate the permeability of NH-modified lithium silicate impregnations: non-heated concrete, and the 650°C-heated concrete that was considered as fire-damaged concrete, respectively. The purpose of using the heated concrete was to confirm if the NH-modified lithium silicate impregnation can penetrate into the heated concrete or not for suggesting a method of repairing fire-damaged concrete in the future. The temperature was set at 650°C because it is higher than the Ca(OH)$_2$ decomposition temperature, and because heating above 650°C will degrade concrete so severely that it is difficult to repair. A small electric furnace was used for the heating, and the heating regime is shown in **Fig. 1**. The temperature was raised to the target temperature (650°C) at a rate of 2 to 3°C/min. and then maintained at the target temperature for 5 hours. After heating, the specimens were left
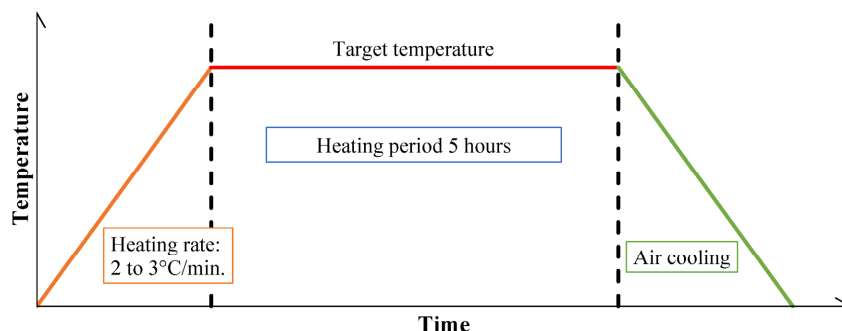

Fig.1 Heating regime of concrete.

in the electric furnace and cooled naturally until they reached room temperature. By using a sufficiently slow heating rate and keeping a long time at the target temperature, it was ensured that the interior of the specimens reached the target temperature. After heating, the specimens were stored in the room at 20±3°C, R.H. 60±5% for about 28 days before immersing in the NH-modified lithium silicate impregnations.

2.3 Permeability evaluation

Masses of the specimens were first measured, followed by placing them in a container filled with the impregnation solution to ensure a complete immersion of the entire specimen for 3 days, as shown in **Fig. 2**. Subsequently, the specimens were removed from the container, and their surfaces were wiped with a dry cloth. Then their masses were measured again. The mass increase ratio, calculated from the mass change before and after immersion, was used as a measure of permeability. Next, the specimens were split using a universal testing machine or cut at the center of the long axis of specimen using a concrete cutter, and the penetration depth of impregnation solution was measured on the fractured section or cutting section according to color change. The penetration fronts of the impregnation solutions can be identified by visual inspection based on the color change of the freshly split section. When the impregnation solution penetrates into the concrete, the concrete color becomes dark. The distance from the concrete surface to the point where the color transitions from dark to light is considered as penetration depth. The penetration depth was measured at four different locations, and the average value was used as the experimental result.

The color change of concrete may be caused only due to water absorption, which does not mean that LS, the effective ingredient of the impregnation solution has entered the concrete specimen. Therefore, in order to investigate the effective permeability of impregnation solution, we conducted SEM-EDS analysis and ICP-AES (Inductively Coupled Plasma Atomic Emission Spectroscopy) analysis to confirm the penetration position of LS and NaOH.

The samples used for the SEM-EDS analysis were collected from the specimens immersed in the impregnation solution with Na/Si molar ratio of 1.25 (Series 1.25). The analysis was carried out using matrix cement paste of

concrete, thus care was taken to avoid the areas with aggregates in the sample collection. The samples were collected within 10 mm of the specimen's surface layer and at the central of the specimen, respectively. The EDS analysis was focused on the Na and Si elements, which are the primary components of the impregnation solution. As a comparison, the SEM-EDS analysis was also performed for the specimen immersed in water. Before the SEM-EDS analysis, all the samples were embedded in Epofix Resin, then cut and polished.

The solid samples, used to prepare the solution for the ICP-AES analysis, were gathered from the surface layer of cylindrical specimen with 100 mm diameter (within 10 mm from the surface), intermediate layer (within 10-30 mm from the surface), and central region (within 30-50 mm from the surface). These solid samples were pulverized into the sizes ranging from 150 to 300 μm, mixed with a standard buffer solution (pH 4.01) at a liquid-solid ratio of 10, and subjected to ultrasonic agitation at 28 kHz for 10 minutes. Subsequently, the mixture solution was filtered through qualitative filter paper with a maximum opening size of 10-15 μm, which conforms to Japanese Industrial Standard JIS P 3801. The liquid that passed through the filter paper was further diluted 100 times with deionized water, and this diluted solution was used in the ICP-AES analysis. The calibration curve for the ICP-AES analysis was prepared within the element concentration range of 0.05-10 ppm.
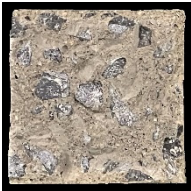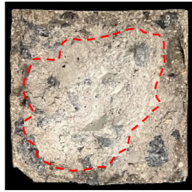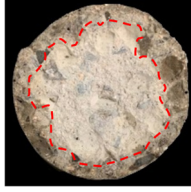
2.4 Experimental results and discussion
2.4.1 Visual inspection and mass change
Table 5 presents the cross-section photographs of the test specimens of G20 after the immersion in each impregnation solution shown in **Table 1**, and describes the penetration situation of impregnation solution, judged visually from the color change of test specimen. **Figure 3** illustrates the mass gain ratios of the test specimens after the immersion. For the unheated test specimens immersed in the solutions of Series 0.00 having only LS, and Series 1.25-30 having a higher solid concentration of 30%, there was no color change on the cross-section of the test specimen, and the mass increase ratio was low. This suggests that the two solutions remained at the surface layer, and thus did not infiltrate the interior of the specimens.

Conversely, for the six solutions with Na/Si molar ratios ranging from 0.25 to 1.75 (Series 0.25 to Series 1.75), the central region of the specimens appeared moist with a visible color change. It can be seen from **Fig. 3**, with increasing Na/Si molar ratio, i.e., increasing the NaOH dosage, the mass gain increased significantly up to a Na/Si molar ratio of 0.75, beyond which the increase became slow. When the Na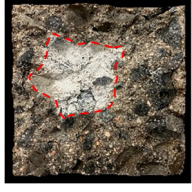/Si molar ratio was in the range of 0.75-1.75, the mass increase ratio was about 4%, which was comparable to the increase ratio in the case of the water immersion (3.99%). This suggests that the permeability of impregnation solution is comparable to that of water when the NaOH is mixed to make the Na/Si molar ratio exceed 0.75. However, though the Na/Si molar ratio was 1.25, the large solid concentration of the so-

Fig. 2 Immersion of specimens into impregnation solution.

Table 5 The color of cross-sections of G20, G40 specimens after immersion in the impregnation solutions with 0.00-1.75 of Na/Si mole ratio for 3 days.

(a) Non-heated concrete specimen

Series	0.00 (G20)	0.25 (G20)	0.50 (G20)	0.75 (G20)	1.00 (G20)
Color of cross-section					
Penetration situation	No color change	Full section	Full section	Full section	Full section
Series	1.25 (G20)	1.75 (G20)	1.25-30 (G20)	NH-only (G20)	1.25 (G40)
Color of cross-section					
Penetration situation	Full section	Full section	No color change	Full section	Full section

(b) Concrete specimen heated to 650°C

Series	0.00 (G20)	0.25 (G20)	0.50 (G20)	0.75 (G20)	1.00 (G20)
Color of cross-section					
Penetration situation	Not reached the center	Full section	Full section	Full section	Full section
Series	1.25 (G20)	1.75 (G20)	1.25-30 (G20)	0.00 (G40)	1.25 (G40)
Color of cross-section					
Penetration situation	Full section	Full section	Not reached the center	Not reached the center	Full section

Note: The penetration situation was a visual evaluation.

lution resulted in a reduced permeability (see Series 1.25-30). If the solid concentration is not high, i.e., water content is suitable, NH-modified LS solution can penetrate into the inside of high-strength concrete [see Series 1.25 (G40) in **Table 5**]. Series NH-only exhibited a significant color change extending to the center, which suggests that 10M NaOH solution has a high permeability.

On the other hand, for the heated specimens the impregnation solutions exhibited higher permeability, compared to the non-heated specimens. Even Series 0.00, which had only LS, displayed a significant color change in an area of approximately 15 mm deep. This is because heating made concrete porous. However, the mass increase ratio of Series 0.00 was still lower than other solutions, indicating that for facilitating the penetration of LS solution into the interior of concrete, the addition of NaOH is necessary even for heated concrete. For the solutions with Na/Si molar ratios ranging from 0.25 to 1.75, the color change ex-

tended to the center of the specimens, accompanied by a high mass increase ratio, similar to that observed in the case of water immersion (9.95%). This suggests that even a small amount of NaOH addition can significantly increase the permeability of LS solution. However, Series 1.25-30 solution with the 30% solid concentration did not reach the center of the G20 concrete specimen. Therefore, the preparation of highly permeable LS surface impregnation requires the appropriate addition of both NaOH and water.

2.4.2 Element distributions of sodium and lithium

The SEM-EDS images at 500 magnification of the un-heated G20 concrete specimens are presented in **Fig. 4**. In the images, the spots of element analysis are shown by cross markers. The elemental analysis results through SEM-EDS are shown in **Fig. 5**. From the specimen immersed in water, sodium (Na) elements were not detected. However, from the surface to the
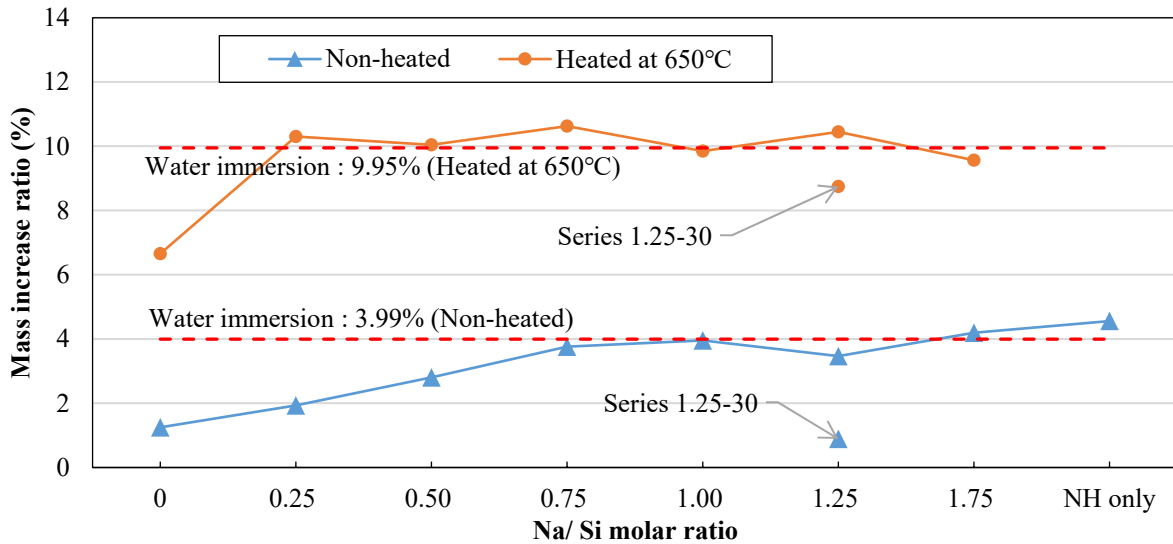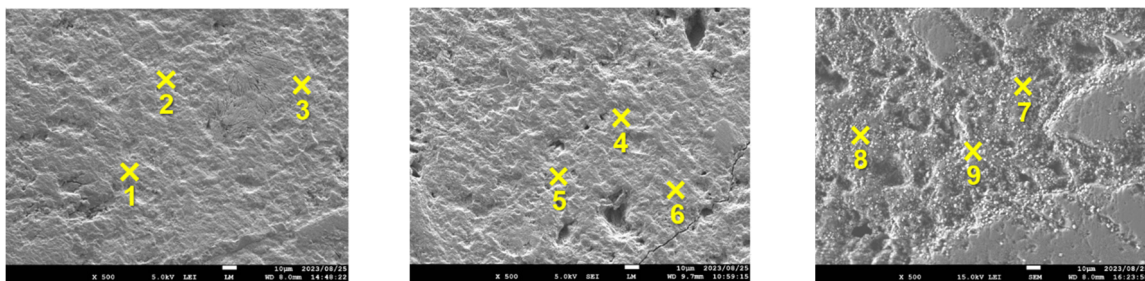

Fig. 3 Mass gain of the G20 specimens after immersion in the impregnation solutions for 3 days.

(a) Water　　　　　　(b) Series 1.25 solution (surface)　　　　　(c) Series 1.25 solution (center)

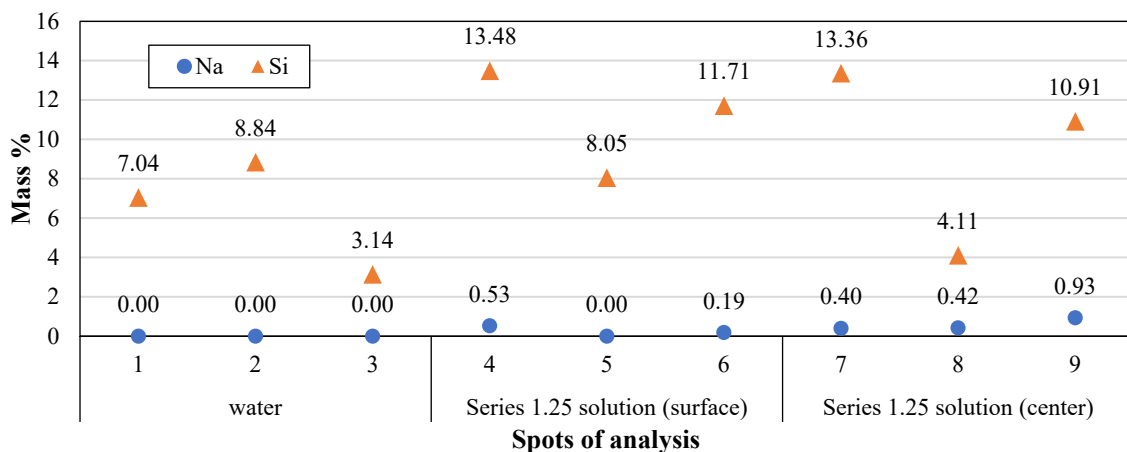Fig. 4 Spots of EDS point analysis for the unheated G20 concrete specimen.

Fig. 5 Distribution of Na, Si elements in the unheated G20 concrete specimens.

center of the specimen immersed in the solution with a Na/Si molar ratio of 1.25, Na elements were detected. It's worth noting that the concentration was very low, and in some points, Na element was not detected.

Silica (Si) was detected in the specimens immersed either in water or in Series 1.25 solution, which is due to the fact that the concrete itself contains silica. Although there are large distribution errors in the content of Na and Si elements, a general trend was found to show that the concrete immersed in the Series 1.25 solution had more Si elements on the surface and in the interior than the concrete that was immersed in water. Therefore, it can be concluded that the NH-modified LS solution indeed penetrated into the interior of the unheated concrete. It can also be inferred from the quantity of Si elements that the effective ingredient (Si) penetrating into the center of the unheated specimen was less than that at the surface layer.

The spots of EDS point analysis for the G20 concrete specimens, which were heated at 650°C and immersed in water or the Series 1.25 solution, are presented in **Fig. 6**. And the EDS analysis results are shown in **Fig. 7**. In both the heated specimens immersed in water and the Series 1.25 solution, Na elements were detected, whereas the specimen immersed in the Series 1.25 solution exhibited higher Na concentration than that immersed in water, with 1.22% to 1.52% at the surface layer and 0.94% to 1.48% in the center. Additionally, Si elements were more prominently detected in the specimens immersed in the Series 1.25 solution, compared to the water. Although

there were some errors in the elemental distributions, in general there was almost no difference in the amounts of Si and Na between the surface layer and the interior. This suggests that the components of the NH-modified LS solution penetrated throughout the concrete specimen. Moreover, these results are consistent with the mass gain ratio shown in **Fig. 3**, indicating that NH-modified LS solution has greater permeability in heated concrete, compared to unheated concrete.

Figure 8 shows the results of ICP-AES analysis for the leaching amounts of lithium (Li) and sodium (Na) elements from the matrix cement paste samples, which were collected from the surface layer (<10 mm), 10-30 mm depth, and 30-50 mm depth, respectively, of the concrete cylinders with diameter 100 mm after being immersed in Series 1.25 solution for 3 days. Although Li and Na were detected from the three reference concretes without immersion, the concentrations of Li and Na elements were below 5 ppm, falling in the range of analytical error of the device used.

Li elements were detected from the surface to the center of the concrete immersed in the Series 1.25, demonstrating that NH-modified LS solution can penetrate into the interior of the concrete regardless of whether the concrete was heated or not. However, for the unheated concrete specimens, the deeper the position, the lower the concentration of Li elements. If the compressive strength is from 24 MPa to 42 MPa, concrete strength has almost no effect on the permeability of NH-modified LS solution.
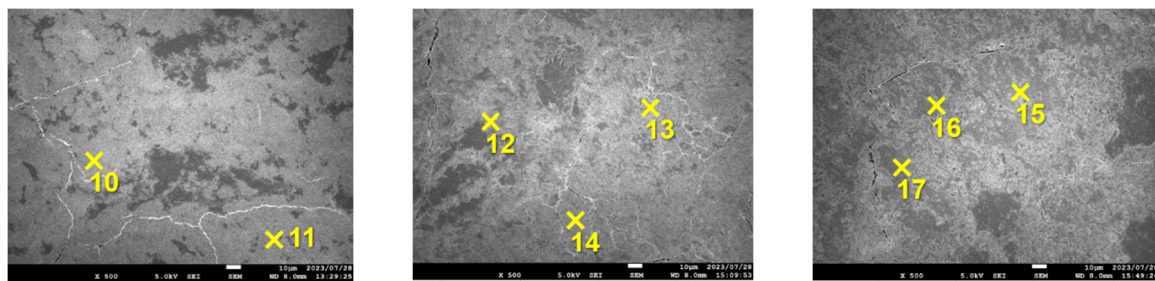
(a) Water   (b) Series 1.25 solution (surface)   (c) Series 1.25 solution (center)

Fig. 6 Spots of EDS point analysis for the G20 concrete specimen heated at 650°C
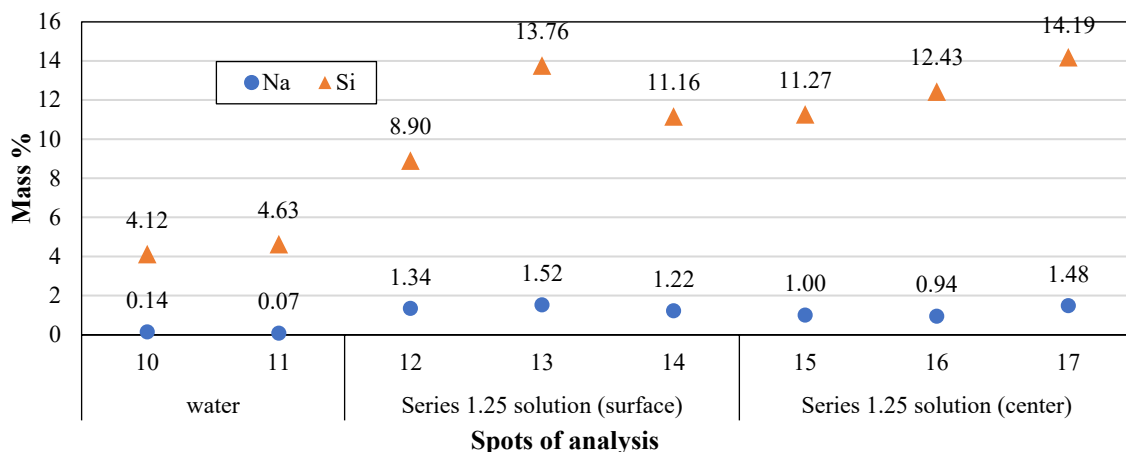

Fig. 7 Distribution of Na, Si elements in the G20 concrete specimens heated at 650°C.
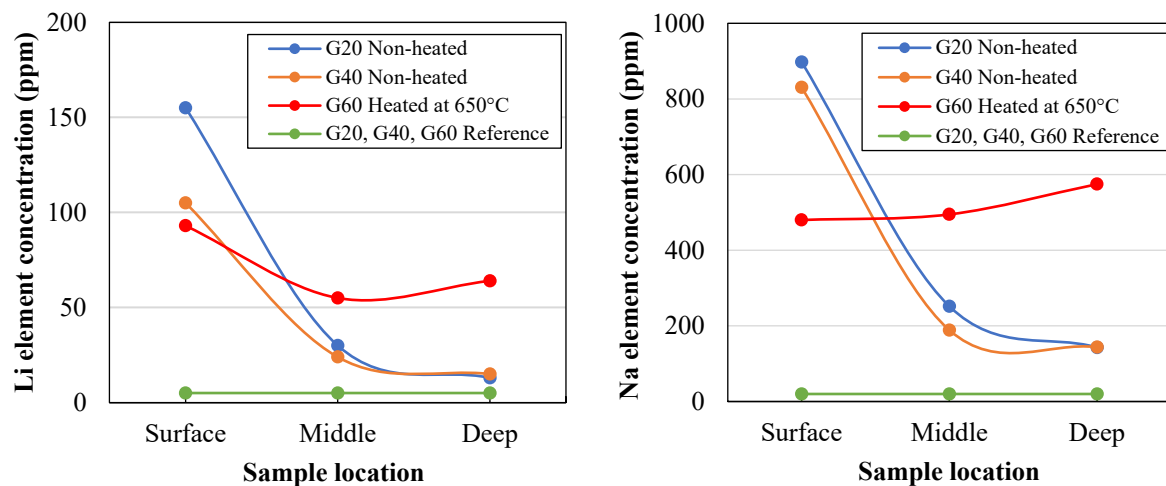
Fig. 8 Element leaching from the concrete samples collected at different locations (ICP-AES analysis).

The detection amount of Li elements from the surface layer of G60 concrete heated at 650°C was nearly the same as the unheated G40 concrete, but the detection amounts in the middle and deep positions of G60 were more than those in G20 and G40. This is because the concrete had more cracks and became porous due to heating. In other words, the higher the degree of concrete deterioration, the greater the permeability of NH-added LS solution. For the unheated specimens, the distribution of Na elements followed the same trend as Li elements. For the heated G60 concrete, the amounts of Na elements from the deep position to the surface layer did not change, with more Na elements detected than the unheated specimens at the same positions. However, Na elements were more detected than Li elements. This is likely because Li elements are continuously bounded to the remaining Si^{4+} of LS, which is not combined with Ca^{2+}, thus are less to leach out than Na elements.

3. High permeability mechanisms of NH-modified silicate solution

One of the reasons that prevents the silicate-based surface impregnation materials from penetrating deeper into concrete is estimated to be the fact that initial reaction between silicate ions and calcium hydroxide in concrete produces calcium silicate, which densifies the concrete and makes the impregnation materials difficult to penetrate further. In addition, judging from the fact that the penetration depth of silicate-based impregnation materials is only a few millimeters, it is estimated that another reason is that the reaction between silicate-based surface impregnation materials and calcium hydroxide is so fast that a layer of calcium silicate is rapidly generated in the surface layer of concrete. For clarifying high permeability mechanisms of NH-modified silicate solutions, we investigated $Ca(OH)_2$ residual ratio in the hardened pastes, prepared from $Ca(OH)_2$ chemicals or either of the two crushed powder of hardened cement paste and different

NH-modified LS solutions, using Thermogravimetry / Differential Thermal Analysis (TG-DTA), and investigated the change of crystalline substances in the hardened pastes by X-Ray Diffraction (XRD) analysis. Additionally, the rate of reaction of the LS solution with the $Ca(OH)_2$ of hardened cement might influence the penetration of the LS solution in concrete. To investigate this reaction rate, we measured the setting time of the mixtures of the crushed powders of hardened cement paste and the NH-modified LS solutions with different Na/Si mole ratios.

3.1 TG-DTA and XRD analysis
3.1.1 Sample preparation and analysis
Hardened pastes were crushed and used for the TG-DTA and XRD analysis. As shown in **Fig. 9**, the hardened pastes were produced by mixing the LS solutions with different Na/Si mole ratios and one of the three kinds of powder: the purchased $Ca(OH)_2$ chemicals (purity 96%, referred to as ch here), the hardened cement paste (referred to as cp here), and the heated cp (referred to as cp 650 here). The cp was produced by mixing ordinary Portland cement and water with a water-cement ratio of 0.50 by mass. After setting, it was sealed and then cured at 60°C till 14 days. Next, a portion of it was coarsely crushed with a hammer and further ground with a ball mill until it reached a specific surface area (Blaine value) of about 6000 cm^2/g. Another portion of the cp was heated to 650°C following the heating regime outlined in **Fig. 1**, and then crushed and ground to be about 6000 cm^2/g of Blaine value. That is, the cp 650 was obtained by heating the cp and grinding it afterwards.

The mix proportions of the mixtures using the powders (cp, cp650, ch) and the NH-modified LS solutions are presented in **Table 6**. Each sample of the ch series, cp series and cp650 series had the same Na/Si ratio. The content of 10 M NaOH aqueous solution was adjusted to make Na/Si ratio varying from 0.00 to 2.25. In addition, each sample of the ch and cp series had the same Ca/Si ratio, but the Ca/Si ratio of the cp650 series was smaller.

Table 6 Mix proportions of the pastes of the powders and the NH-modified LS solutions.

Sample ID	Mix proportions (mass ratio)			Molar ratio	
	Powder	Solution preparation		Na/Si	Ca/Si
		Lithium silicate	Sodium hydroxide		
cp-0.00	100.00 (Cement paste)	59.06	0.00	0.00	1.41
cp-0.25			1.97	0.25	
cp-0.50			3.93	0.50	
cp-0.75			5.90	0.75	
cp-1.00			7.86	1.00	
cp-1.25			9.83	1.25	
cp-1.75			13.76	1.75	
cp-2.25			17.69	2.25	
cp-NH		H₂O: 45.48※	9.83	-	-
ch-0.00	100.00 (Ca(OH)₂)	287.51	0.00	0.00	1.41
ch-0.25			9.57	0.25	
ch-0.50			19.14	0.50	
ch-0.75			28.71	0.75	
ch-1.00			38.28	1.00	
ch-1.25			47.85	1.25	
ch-1.75			66.98	1.75	
ch-2.25			86.12	2.25	
ch-NH		H₂O: 221.38※	47.85	-	-
cp650-0.00	100.00 (Cement paste heated at 650°C)	59.06	0.00	0.00	0.88
cp650-0.25			1.97	0.25	
cp650-0.50			3.93	0.50	
cp650-0.75			5.90	0.75	
cp650-1.00			7.86	1.00	
cp650-1.25			9.83	1.25	
cp650-1.75			13.76	1.75	
cp650-2.25			17.69	2.25	
cp-NH		H₂O: 45.48※	7.86	-	-

※The amount of water included in the lithium silicate used in the paste with a Na/Si of 1.25 was used.

This is because the Ca/Si calculations only considered the Ca in Ca(OH)$_2$. The Ca(OH)$_2$ in the hardened cement paste powder used in cp650 series decomposed due to heating. The amount of Ca(OH)$_2$ was estimated by TG-DTA analysis from the weight loss in the range of 400 to 500°C, using Eq. (2). The heating rate was 10°C/min.

$$Ca(OH)_2 = weight\ loss\,(\%) \times \frac{Ca(OH)_2 \cdot 1\ mol\ [g/mol]}{H_2O \cdot 1\ mol\ [g/mol]} \quad (2)$$

After mixing the pastes of the NH-modified LS solution and the powder, they were stored in airtight containers at 20°C. To measure the time-dependent change of Ca(OH)$_2$ residual ratio in the hardened pastes, the hardened pastes were immersed in acetone to stop the reaction after 10 minutes, 3 hours, 6 hours, 24 hours, and 7 days from the start of mixing. Subsequently, suction filtration was performed, and the hardened pastes were dried at 60°C for 2 hours. However, Series ch-NH, where the 10 M NaOH solution and water were mixed with the Ca(OH)$_2$ chemicals, did not set and remained in a paste state. Thus, the samples of the Series ch-NH were dried at 105°C. All the dried samples were stored in sealed containers until the TG-DTA and XRD analysis.

The quantitative analysis of residual Ca(OH)$_2$ was performed in the same way as that of powder's Ca(OH)$_2$ amount described above. The crystalline components in the hardened pastes with the reaction time of 7 days were investigated by XRD analysis. The XRD analysis used the Rigaku SmartLab 9 kW model and adopted the powder method. The measurement conditions included the use of CuKα radiation, a tube voltage of 45 kV, a tube current of 200 mA, and a scan speed of 10°/min.

3.1.2 TG-DTA analysis results
The results of TG-DTA are shown in **Fig. 10**. In the three series, marked as ch, cp, and cp650, the powders used were the Ca(OH)$_2$ chemicals, the cp powder, and the cp 650 powder, respectively. And initial Ca(OH)$_2$ contents

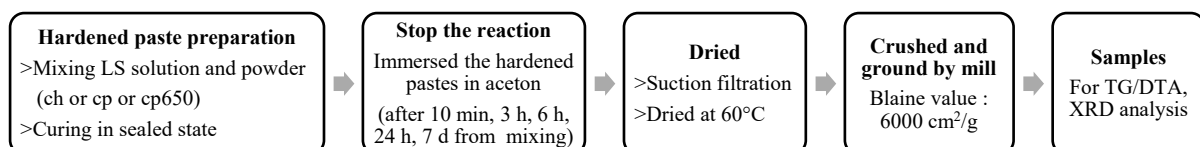| Hardened paste preparation	Stop the reaction	Dried	Crushed and ground by mill	Samples
>Mixing LS solution and powder (ch or cp or cp650) >Curing in sealed state	Immersed the hardened pastes in aceton (after 10 min, 3 h, 6 h, 24 h, 7 d from mixing)	>Suction filtration >Dried at 60°C	Blaine value : 6000 cm²/g	For TG/DTA, XRD analysis

Fig. 9 The preparation of samples used for the TG-DTA and XRD analysis.

of three series were taken as 100%.
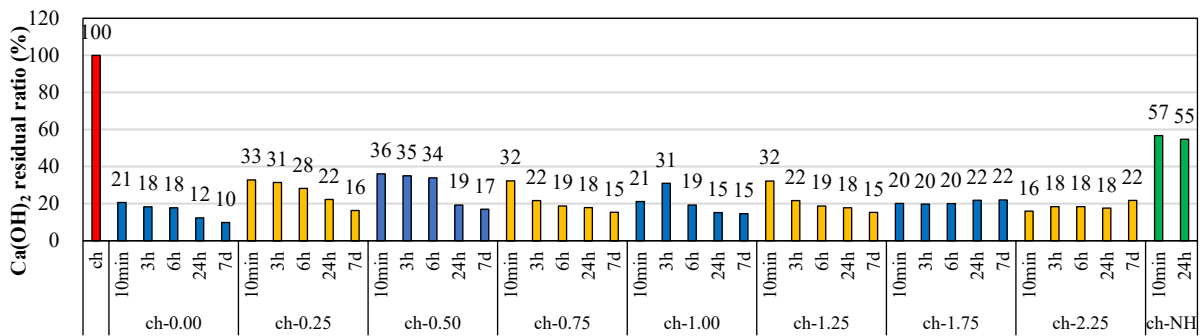
(1) cp series

As shown in **Fig. 10(a)**, for Sample cp-0.00 without NH addition, the $Ca(OH)_2$ residual ratio decreased to 52% after 10 minutes of the reaction described in Eq. (1), indicating that $Ca(OH)_2$ was rapidly consumed by the reaction. Although $Ca(OH)_2$ residual ratio gradually decreased thereafter, it remained at 43% after 7 days, suggesting that the reaction consuming $Ca(OH)_2$ mostly occurred within the first 10 minutes from mixing. On the other hand, for the samples using a blending solution of NaOH and LS (Samples cp-0.25 to cp-

2.25) and experiencing 10 minutes of the reaction, retained a higher $Ca(OH)_2$ residual ratio than the Sample cp-0.00, ranging from 77% to 95%, and the decrease of $Ca(OH)_2$ was gradual over a period of 7 days. When the Na/Si molar ratio was between 0.50 and 1.25, there was no large difference in the $Ca(OH)_2$ residual ratios of the four samples with different reaction times.

For the Sample cp-1.75 and the Sample cp-2.25, even after 7 days, the $Ca(OH)_2$ residual ratio still remained high at 77% and 80%, respectively. This suggests that when overmixed with NaOH, the reaction described in Eq. (1) was significantly inhibited. However, when the Na/Si molar ratio was 0.5 or more, the $Ca(OH)_2$ residual ratio was more than 81% in the samples of cp series with
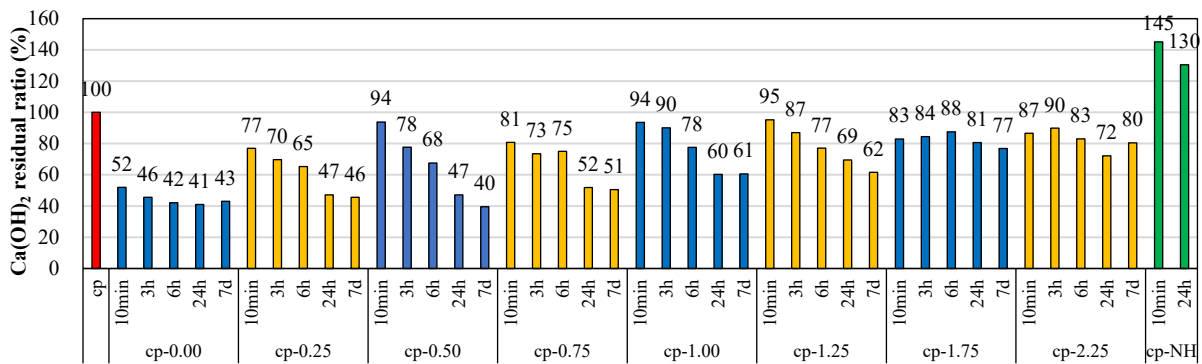
(a) cp series

(b) ch series
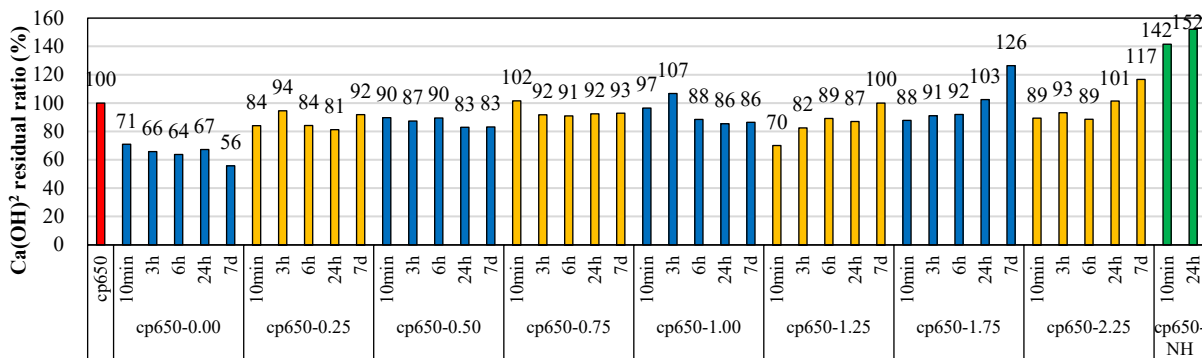
(c) cp-650 series

Fig. 10 Amount of residual $Ca(OH)_2$ in each hardened paste: Results of TG-DTA analysis.

reaction time of 10 minutes.

(2) ch series

As shown in **Fig. 10(b)**, the $Ca(OH)_2$ residual ratio of ch series showed a similar trend to that of the cp series, i.e., the NaOH addition increased the $Ca(OH)_2$ residual ratios of the samples of ch series with reaction time of 10 minutes. However, the $Ca(OH)_2$ residual ratios of the ch series were smaller than the cp series for the same Na/Si ratio and for the same reaction time (10 minutes). This is because the $Ca(OH)_2$ chemicals could come into direct contact with the LS solution immediately after mixing, whereas the $Ca(OH)_2$ distributed in the hardened cement powder (particles) required time to contact with the LS solution.

For the Sample ch-1.75 and the Sample ch-2.25, the reaction was almost stopped from 10 minutes to 7 days, thus the $Ca(OH)_2$ residual ratios in the two samples did not decrease. After the two samples experienced the 10-minute reaction, there was little $Ca(OH)_2$ remaining, and the NaOH probably reached a saturation concentration that prevented the reaction between $Ca(OH)_2$ and the LS.

(3) cp650 series

As shown in **Fig. 10(c)**, for the reaction time of 10 minutes, the $Ca(OH)_2$ residual ratios of the samples of cp650 series samples with NaOH addition, had not a certain trend with the increase of Na/Si mole ratio, not like the Sample cp650-0.00. Also, the pattern of $Ca(OH)_2$ residual ratio varying with the reaction time more than 10 minutes was different from those of the cp and ch series. After 10 minutes, the $Ca(OH)_2$ residual ratio increased with the reaction time.

Additionally, we similarly found that the $Ca(OH)_2$ residual ratio decreased with increasing the reaction time in the cp-NH sample and the ch-NH samples, but increased with increasing the reaction time in the cp650-NH sample, which were mixed only the 10 M NaOH solution. However, for the ch-NH samples, $Ca(OH)_2$ residual ratios did not exceed 100% of its initial value. In contrast, the cp-NH samples and the cp650-NH samples had $Ca(OH)_2$ residual ratios exceeding 100%. Kim *et al.* (2016) also reported this phenomenon and explained that NaOH caused the leaching of Ca^{2+} from the hydrates of cement besides $Ca(OH)_2$.

3.1.3 XRD analysis results
(1) cp series and cp650 series

XRD patterns of the samples of the cp series and the cp650 series are presented in **Fig. 11(a)**. Compared to the raw cp powder, the cp650 powder exhibited lower peaks of portlandite ($Ca(OH)_2$) and lower hump around $2\theta=29°$, but had more tobermorite to be detected, which has a lower Ca/Si ratio than C-S-H gel. The hump at about 29° represents the presence of amorphous phase C-S-H, and the broad hump of C-S-H overlaps with $CaCO_3$ peak at about 29.2°. From all the cp-xx and cp650-xx samples, where xx is 00, NH, 0.75, 1.25 or 2.25, little calcite ($CaCO_3$) were detected. The $CaCO_3$ was generated due to

carbonation during the preparation (crushing and grinding) of the cp and cp650 powders, and the preparation of XRD samples of cp-xx and cp650-xx in the air.

AFm was observed from the cp powder and the five cp-xx samples of hardened paste using the cp powder. This is because that the hydration reaction of C_3A or C_4AF in Portland cement produces AFt at short age, which is further converted to AFm at long age. And an aqueous NaOH solution with a molar concentration of 2 M or more is mixed, ettringite disappears and gets replaced by the AFm phase [i.e., $NaCa_4Al_2O_6(SO_4)_{1.5} \cdot 15H_2O$)] and amorphous aluminum-hydroxide (Gijbels *et al.* 2020).

But the AFm peaks disappeared, and β-C_2S were detected from the cp650 powder and the five cp650-xx samples using the cp650 powder. This result indicates that almost all of the AFm as well as some of the $Ca(OH)_2$ and C-S-H gels in the cp650 powder decomposed during the heating at 650°C (Daiki *et al.* 2021).

The cp-NH and cp650-NH samples showed increased $Ca(OH)_2$ peaks, but the CC peak of the cp-NH sample became low, compared to the cp powder and the cp650 powder. Also, disappeared AFm peak in the cp650 powder was not detected from all the cp650-xx samples, as stated above. This indicates that NaOH caused the degradation of C-S-H gels and interfered with the re-hydration of decomposed AFm to precipitate the Ca^{2+} ions that reformed the $Ca(OH)_2$.

The cp-0.00 sample, mixing LS solution only, had lower peaks of portlandite, compared with the cp powder, and cp-NH, respectively. The cp650-0.00 samples also had lower peaks of portlandite than those of the cp650 powder, and the cp650-NH, respectively. Furthermore, due to the decomposition of C-S-H gels under high temperature (Zhang *et al.* 2013), the halo peak around 30° of the cp650-00 sample was lower than that of the cp-0.00 sample. However, from the fact that the halo peaks of the cp650-00 and the cp-0.00 samples were higher than those of the cp650 powder, cp650-NH, and cp powder, cp-NH, respectively, it was judged that $Ca(OH)_2$ was reacted with lithium silicate to form C-S-H gels, as described in Eq. (1).

However, for the cp-yy and the cp650-yy samples with Na/Si mole ratio of 0.75 to 2.25 (yy is 0.75 or 1.25 or 2.25 here), no matter if the used powder was heated or not, the peaks for portlandite were higher than those of the cp-0.00 and cp650-0.00 samples, and increased as the Na/Si molar ratio increased. Also, between $2\theta=25$ to 35°, the cp-0.00 sample exhibited the largest hump that represents C-S-H gels. The cp-0.75, 1.25 and 2.25 samples also had the humps, that were lower than that of the cp-0.00 sample, but were higher than those of the cp powder and the cp-NH sample. This result suggests that even if the NaOH was added into the LS, the LS can react with $Ca(OH)_2$, but the reaction was decreased.

For the cp650-0.00, 0.75, 1.25, 2.25 samples, it can be found that with increasing the Na/Si mole ratio, the portlandite peaks at 18°, and 34° became high, but the portlandite peak at about 28.8° disappeared from the samples,

which was observed in the cp650-NH sample. The difference can not be clearly observed for the CC peaks of cp650-yy samples, though the CC peak of the cp650-0.00 sample was the lowest. However, the cp650-0.00 showed the highest tobermorite peak at about 32.2°, which is a kind of C-S-H with low Ca/Si, and the highest β-C_2S peak at

about 34°. The tobermorite and β-C_2S peaks of the cp650-0.75, 1.25, 2.25 samples became lower and lower with increasing the Na/Si mole ratio. Compared with the raw cp650 powder, the five cp650-xx samples had lower tobermorite peaks at about 32.2° and lower β-C_2S peaks at about 34°. At present, the reasons are unknown. The presence of

(a) cp series and cp650 series

(b) ch series
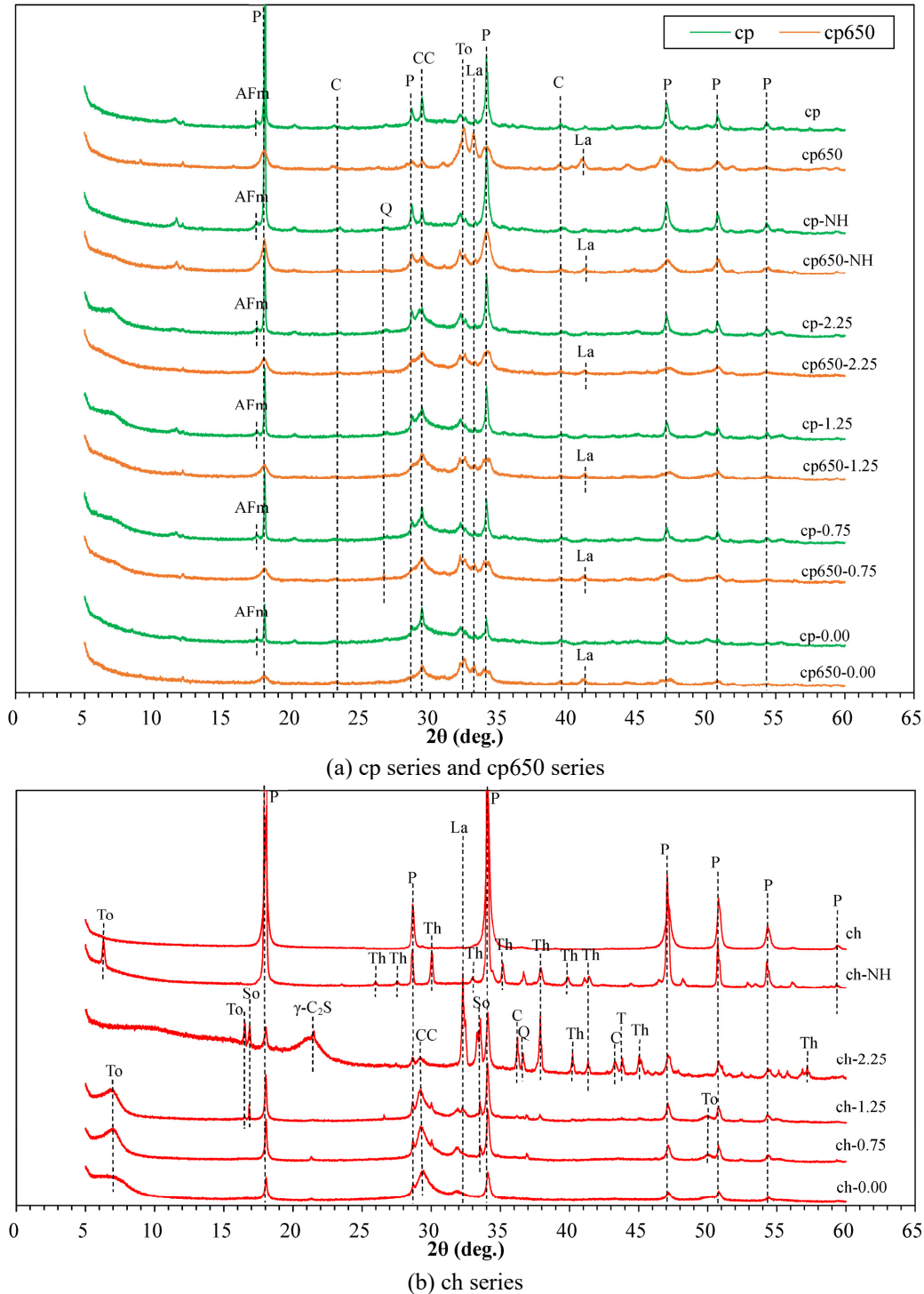
P: Portlandite; To: Tobermorite, C-S-H; Th: $Na_2CO_3(H_2O)$; So: Sodium calcium silicate, N-C-S-H; C: Calcite, $CaCO_3$; Q: quartz, SiO_2; CC: C-S-H, Calcite; La: β-C_2S.

Fig. 11 X-ray diffraction analysis results.

NaOH seems to enlarge the decrease of tobermorite and β-C_2S in cp650-yy samples. The less the formation of tobermorite and β-C_2S, the easier the penetration of LS solution.

(2) ch series
XRD patterns for the $Ca(OH)_2$ powder (ch) and the five hardened pastes (ch-xx) prepared by the $Ca(OH)_2$ powder and either of the five kinds of solution are shown in **Fig. 11(b)**. The $Ca(OH)_2$ powder, of course, only exhibited several portlandite peaks. Na_2CO_3 was detected from the ch-NH sample due to the carbonation occurring during the preparation and store of this paste. The ch-0.00 sample had a hump around 30° and had lower portlandite peaks than the $Ca(OH)_2$ powder (ch). Like as the cp-0.00 and the cp650-00, the calcium silicate reaction was confirmed. The ch-1.25 and the ch-0.75 showed higher portlandite peaks than the ch-0.00. The two samples' portlandite peak intensities were almost the same, which agrees with the trend of TG-DTA results shown in **Fig. 11(c)**. This is due to that in the ch-1.25 sample, sodium calcium silicate was also detected at about 17°, i.e., more Ca^{2+} was consumed than the ch-0.75 sample. However, with increase Na/Si mole ratio from 0.00 to 1.25, the hump became lower, indicating the calcium silicate reaction decreased.

Although there was almost no hump around 30° in the ch-2.25 sample sodium calcium silicate, γ-C_2S, tobermorite, and calcite were detected in large amount besides Na_2CO_3, of which the generation consumed NaOH or $Ca(OH)_2$, or the two. Hence, the ch-2.25 sample showed lower portlandite peaks at 18° and 34° than the ch-0.75 and ch-1.25 samples so that the $Ca(OH)_2$ residual ratio was small, as shown in **Fig. 11(c)**.

The reaction occurred in the ch-1.25, 2.25 samples were complicated, the formation of sodium calcium silicate, etc. resulted in that the $Ca(OH)_2$ residual ratios of the ch-1.25, 2.25 samples were lower than that of the ch-0.75 sample. In the cp-1.25, 2.25 sample sodium calcium silicate and γ-C_2S were not detected by the XRD analysis. This is because the NH-added LS solution used was less

than the ch-1.25, ch-2.25 samples.

3.2 Setting time test for the mixture of hardened cement powder and NH-modified silicate solution
3.2.1 Mixtures and measurement
The mixtures were prepared by mixing the NH-modified LS solutions with varying Na/Si molar ratios from 0.00 to 1.25 or 2.25, and the cp powder or the cp650 powder. The mix proportions of the mixtures were the same as those used in the TG-DTA and XRD analyses (see **Table 6**).

The penetration test was conducted to measure the final setting, following JIS R 5201 (Physical Testing Methods for Cement). A standard needle with a diameter of 1 mm was used, and the dimension of sample container was 60 mm diameter. The thickness of sample was 30 mm, and the needle penetration was conducted at 10-minute interval after mixture mixing. The elapsed time from mixing the powder and the solution until the depth of penetration became 0 mm was recorded as the final setting time.

3.2.2 Experimental results
The test results for the final setting time of each mixture are presented in **Fig. 12**. The cp-0.00 and cp650-0.00 mixtures, which used the LS solution only, hardened during mixing, and thus the final setting time was recorded to be 0 minutes. In contrast, other mixtures with NaOH addition did not set immediately after mixing, having longer setting times than the cp-0.00 and the cp650-0.00 mixtures.

When focusing on the effect of the amount of NaOH blend, it can be found that the final setting time varied in three stages with increasing Na/Si molar ratio, regardless of whether the cp powder or the cp650 powder was used. Up to a certain value of Na/Si molar ratio, the increase of blended NaOH led to a prolongation of setting time. When the molar ratio of Na/Si was at the intermediate level, the setting time hardly varied with the NaOH dosage. However, the Na/Si molar ratio was increased above a certain value, the increase of blended NaOH, on the
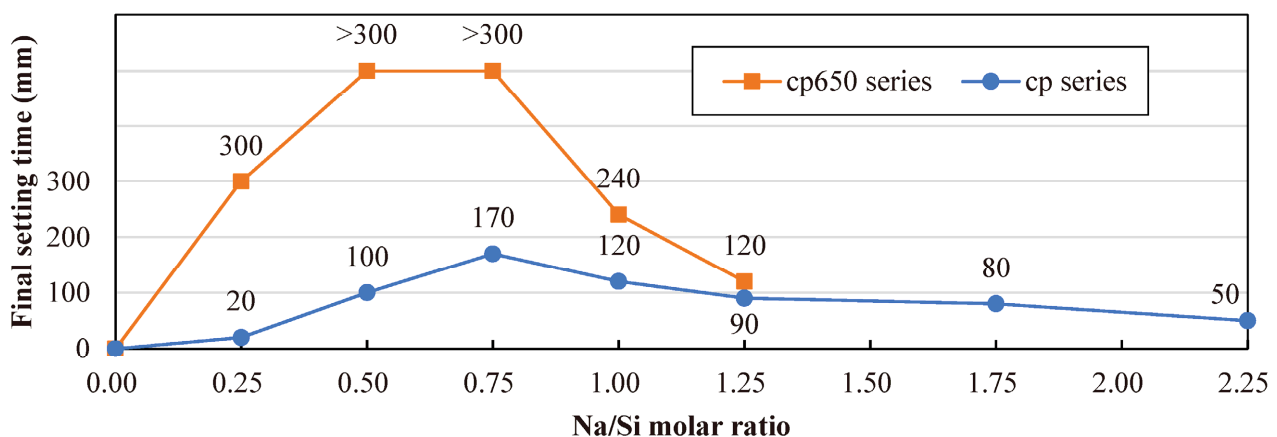
Fig. 12 Final setting time of each mixture of hardened cement paste powder and NH-modified LS solution.

contrary, caused a decrease of setting time.

It's worth noting that for the mixtures using the cp650 powder, when the Na/Si molar ratios were 0.50 and 0.75, the final setting times were over 300 minutes. Since the Si/Ca molar ratio of the mixtures using the cp650 powder was smaller than that of the mixtures using the cp powder, in the range of Na/Si molar ratios from 0.25 to 1.25, for the same Na/Si molar ratio, the cp650-based mixtures had longer setting times than the cp-based mixtures.

These results indicate that the reaction between silicate in the LS solution and calcium in hardened cement paste was delayed by the addition of sodium hydroxide, whereas adding too much or too little NaOH would reduce the delaying effect. As shown in **Fig. 12**, the NH-modified LS solutions with the Na/Si molar ratio ranging from 0.50 to 0.85 can greatly retard the silicate reaction between LS and calcium in hardened cement paste, thus have high permeability in concrete. Depending on the denseness of concrete and the desired depth of penetration, Na/Si molar ratios above 0.85 are acceptable.

4. Discussion

Pallagi *et al.* (2012) investigated the solubility of $Ca(OH)_2$ in aqueous NaOH solutions up to 12.50 mole at 25°C, and found that the solubility of $Ca(OH)_2$ steadily decreases with the increasing NaOH concentration. The NaOH addition decreased the solubility of $Ca(OH)_2$, thus reduced the reaction of the $Ca(OH)_2$ of hardened cement paste or chemicals with the lithium silicate (LS) solution. This caused the $Ca(OH)_2$ residual ratios of the cp-xx and ch-xx samples (xx>0.00) remaining at a higher level, compared to the cp-0.00 sample, and the ch-0.00 sample mixing the LS solution only, respectively. With the elapsed time, calcium hydroxide gradually dissolves and reacts with LS. As a result, the $Ca(OH)_2$ residual ratios of the cp-xx and the ch-xx samples (xx>0.00) decreased with the increase of reaction time from 10 minutes to 7 days, like the cp-0.00 and the ch-0.00 samples. XRD analysis also confirmed that the cp-xx and the ch-xx samples that added the NaOH solution had more $Ca(OH)_2$ than the cp-0.00 sample and the ch-0.00 sample, and the residual $Ca(OH)_2$ in the cp-xx samples increased with the increase of Na/Si mole ratio, as shown in **Fig. 11**. Therefore, with the increase of Na/Si mole ratio up to 0.75, the silicate reaction between the cp powder and the NH-added LS solution decreased, and thus the final setting time became long, as shown in **Fig. 12**. The less reaction between $Ca(OH)_2$ and LS solution, the fewer the products and the easier the penetration of the LS solution. And the longer the setting time, the more time LS solution has to penetrate, thus increasing the depth of penetration.

The addition of NaOH increases the pH of pore solution, which increases the solubility of ettringite. Bizzozero *et al.* (2014) and Alahrache *et al.* (2016) reported that higher pH values in the pore solution lead to a destabilization of ettringite. C-S-H gel also decomposes under high-alkalinity condition to form quartz and $Ca(OH)_2$

(Martinez-Ramirez and Palomo 2001a, 2001b; Walker *et al.* 2016). Quartz was detected from the cp-xx, and cp650-xx samples (xx>0.00), as shown in **Fig. 11(a)**. This is because alkalis of NaOH bound in C-S-H gels, which leads to a structural rearrangement of C-S-H, shortening the silica chains (Yan *et al.* 2022). The cation (Na$^+$) with little ion radius promotes the leaching of calcium from the interlayer, the calcium in C-S-H gels is replaced by sodium (Liu *et al.* 2022; Masoumi *et al.* 2019; Sugiyama 2008). The leaching of calcium resulted in polymerization of silicon-oxygen tetrahedra, increasing the Q^3 and Q^4 sites of $[SiO_4]^{4-}$ in C-S-H dreierketten (Gutberlet *et al.* 2015). Therefore, C-S-H gels have been found to transform into a more ordered tobermorite-like structure during the dissolution process, which naturally led to a decrease in the Ca/Si ratio (Trapote-Barreira *et al.* 2015). Kurumisawa *et al.* (2013) also found that the Ca/Si ratio of C-S-H gels decreased, following silicate polymerization related to the structural transformation of the C-S-H gels.

In this study, more tobermorite was detected in the samples using both NaOH and LS solution than in the three samples without NaOH addition, and sodium calcium silicate was detected by XRD analysis from the ch-1.25 and ch-2.25 samples. Therefore, the transformation of C-S-H gels or/and decomposition of ettringite resulted in that the cp-NH and the cp650-NH had higher $Ca(OH)_2$ residual ratios than the raw cp powder, and the raw cp650 powder, respectively. The higher the concentrations of NaOH, the more the decomposition of ettringite and C-S-H gels. In addition to NaOH hindering the silicate reaction between $Ca(OH)_2$ and LS, the decomposition of ettringite and C-S-H gels by high concentration of NaOH is another reason for the small change in the $Ca(OH)_2$ residual ratios of the cp-1.75 and cp-2.25 samples over time.

The inclusion of Na$^+$ in C-S-H gels may reduce the ability of NaOH inhibiting the silicate reaction. And the Ca^{2+} released due to the decomposition of ettringite and C-S-H gels may increase the silicate reaction, while the hump of XRD patterns of the cp-1.25 and the cp-2.25 had no obvious difference. Therefore, when the Na/Si mole ratio was above 0.85, the setting time of the mixture of the cp powder and the NH-added LS solution became short with increasing the Na/Si mole ratio.

On the other hand, under high temperature above 450°C, $Ca(OH)_2$ in hardened cement paste will decompose to CaO and H_2O. The decomposition of hydrates and the inhomogeneous thermal expansion of matrix cement paste and aggregates due to heating lead to loosening and cracking of concrete. Thus, the concrete exposed to high temperature is easily carbonated (Li and Li 2011; Li *et al.* 2013). During the preparation of the raw cp650 powders, due to the thermal decomposition of $Ca(OH)_2$, the raw cp650 powder had few $Ca(OH)_2$ than the raw cp powder. The former had a lower XRD intensity of $Ca(OH)_2$ than the latter, as described earlier.

Ettringite becomes amorphous from 150°C, and fur-

ther decomposes from 500°C to generate insoluble anhydrite (Kira *et al.* 1981). Therefore, in the raw cp-650 powder ettringite was not detected by the XRD. Dehydrated or decomposed ettringite may rehydrate in a high humidity environment (Kira *et al.* 1981), but the normal formation of ettringite can not take place because gypsum reacts with alkalis to produce sodium sulphate (Martinez-Ramirez and Palomo 2001a, 2001b). For this reason, AFt or AFm were not detected from cp650-xx samples.

Between 100 and 200°C, the dehydration of C-S-H gels occurs (Fares *et al.* 2010; Alarcon-Ruiz *et al.* 2005), and the deterioration of C-S-H has been reported to start when the elevated temperature is higher than 500°C (Zhang *et al.* 2013). C-S-H gels suffer from decomposition when the temperature is higher than 600°C (Jia *et al.* 2019). Xu *et al.* (2023) reported that dreierketten units in C-S-H gels begin to decrease at 550°C, and disappeared at 650°C, associated with a continuous increase of a new amorphous nesosilicate phase. If water is present, C-S-H would be rehydrated and reformed (perhaps only partially) from this amorphous nesosilicate phase. The rehydration and reformation of C-S-H gels makes the concrete exposed to elevated temperature gain strength recovery to some extent (Li and Li 2011).

However, for the hydration of Portland cement, the presence of NaOH leads to a lower Ca/Si ratio (around 1.5) in C-S-H gels, compared to the alkali free system (around 1.7), and thus the precipitation of portlandite is slightly higher (Mota *et al.* 2018). Therefore, the addition of NaOH caused the C-S-H gels in the cp650-0.25 to cp650-1.25 samples, which were deteriorated or decomposed by the 650°C-heating, to reform new type of C-S-H gels with lower Ca/Si ratio by re-hydration, releasing part of Ca^{2+} ions. The released Ca^{2+} ions increased with the reaction time, resulting in an increase of $Ca(OH)_2$ in the cp650-0.25 to cp650-2.25 samples, even the amount of $Ca(OH)_2$ in the cp650-NH sample exceeded that of the raw cp650 powder, as shown in **Fig. 10(c)**.

When the Na/Si mole ratio was in the range from 0.25 to 1.00, the hardened pastes, using the cp650 powder and NH-added LS solution, had more $Ca(OH)_2$ than the cp650-0.00, regardless of reaction time, which was also confirmed by the XRD analysis through comparing the intensities of $Ca(OH)_2$ peaks of the cp650-0.00 and the cp650-0.75. This indicates that the reaction between the cp650 powder and the LS solution was reduced by NaOH like the cp-xx samples and the ch-xx sample (xx>0.00), thus the cp650-0.25 to cp650-1.00 mixtures had long setting time, as shown in **Fig. 12**.

However, when the Na/Si ratio was increased from 1.25 to 2.25, the increase of $Ca(OH)_2$ with the reaction time became small, even the amount of $Ca(OH)_2$ was smaller than that of the cp650-0.00 sample in some cases, as shown in **Fig. 10(c)**. As in the ch-1.25 and the ch-2.25 samples, the complicated reaction, which generated sodium calcium silicate and thermonatrite under high concentration of NaOH, occurred to consume Ca^{2+} and Na^+, thus reduced the residual $Ca(OH)_2$. At the Na/Si ratios

greater than 1.25, the formation of the products such as sodium calcium silicate and thermonatrite promoted the setting of the mixtures of cp650 powder and NH-added LS solution. The Na^+ consumption also weakened the inhibitory effect of NaOH on the participation of $Ca(OH)_2$ in the silicate reaction. Thus, with the increase of Na/Si ratio from 1.25, the setting time of the mixtures became shorter and shorter, as show in **Fig. 12**. Although the mixtures of cp650 powder and NH-added LS solution set fast when the Na/Si ratio exceeds 1.25, the NH-added LS solutions still have higher permeability than the LS solution due to the fact that NaOH delays the reaction between $Ca(OH)_2$ and LS, and thus they can penetrate to the center of the small concrete specimen with 10 cm length of side [see Series 1.25 (G20) and Series 1.75 (G20) in **Fig. 2**].

Carbonation occurred during the sample preparation of the hardened paste made from $CaOH_2$ chemicals and NaOH solution, which resulted in a lower $Ca(OH)_2$ content of the ch-NH sample than the raw $CaOH_2$ chemicals, and the $Ca(OH)_2$ residual ratios of the cp-NH, ch-NH samples with 24-hour reaction time were lower than those of the samples with 10-minute reaction time. We estimate that much carbonation occurred in the storage containers with air during the 24-hour reaction period. However, in NaOH aqueous solution, degraded C-S-H gels were reformed into the new gels with low Ca/Si ratio, and as the amount of reformed C-S-H gels increased, more Ca^{2+} ions were presented to form $Ca(OH)_2$, so that the cp650-NH with 24-hour reaction time had more $Ca(OH)_2$ than the cp650-NH with 10-minute reaction time, even though the former might have more carbonation reactions.

The cp-NH and cp650-NH samples showed the more presence of $Ca(OH)_2$ and the lower hump and lower CC peak at 2θ=29.4°, compared with other cp-xx and cp650-xx samples (xx>0.00). As discussed earlier, the high amount of NaOH disintegrated the C-S-H gels and decreased the solubility of $Ca(OH)_2$, thus $Ca(OH)_2$ was increased in the cp-NH and cp650-NH samples.

5. Summary

In this paper, in order to develop a silicate-based surface impregnation solution with high permeability for surface-to-interior restoration of concrete degraded by general aggressive mediums or fire, the permeability of modified impregnation solution consisting of sodium hydroxide (NaOH), lithium silicate (LS) and water, was evaluated in comparison with traditional lithium silicate solution. The effect of the blending ratio of NH on LS permeability and the mechanism by which the addition of NH improves LS permeability were discussed by impregnation testing and SEM-EDS analysis of concrete, setting time test of the mixtures of hardened cement powder and impregnation solution, as well as XRD and TG-DTA analysis of the mixtures after hardening. The 650°C-heated concrete specimens and the mixtures prepared by mixing

650°C-heated cement paste powder and impregnation solution were also used in these tests and analyses besides the unheated concrete specimens and the unheated cement paste powders. The obtained results are summarized as follows:

(1) When blending NaOH in LS solution at a suitable mole ratio of Na/Si, LS solution exhibited a higher permeability, compared to LS solution only, regardless of whether the concrete was heated. However, if the blending ratio was too large, NaOH would change the hydrates (C-S-H gels and AFm or AFt) of Portland cement to release Ca^{2+} so that promote the reaction between LS and the degraded or reformed hydrates. Appropriate blending ratio of NaOH is such that the Na/Si molar ratio of NaOH-added LS solution is between 0.5 and 1.25.

(2) NaOH addition delayed the reaction between LS solution and the $Ca(OH)_2$ that is one of hydrates of Portland cement, which generates silicate calcium. Slow formation of calcium silicate allows for greater penetration as the LS penetration path is not blocked.

(3) The alkalinity of concrete decreases after subjected to elevated temperature due to the decomposition of $Ca(OH)_2$ and its carbonation during heating and cooling. Repairing of heated concrete using NaOH-added LS solution obviously improves the alkalinity of the heated concrete. Moreover, rehydration of decomposed C-S-H gels in the presence of NaOH results in the formation of new C-S-H gels with lower Ca/Si, compared with original gels, which releases Ca^{2+} to increase $Ca(OH)_2$. The increase in the alkalinity of the heated concrete facilitates the protection of reinforcement.

The strength and durability improvement of repairing fire-damaged concrete and reforming generally degraded concrete using the highly permeable impregnation solution developed in this study will be reported separately in other papers.

References

Alahrache, S., Winnefeld, F., Champenois, J. B., Hesselbarth, F. and Lothenbach, B., (2016). "Chemical activation of hybrid binders based on siliceous fly ash and Portland cement." *Cement and Concrete Composites*, 66, 10-23.

Alarcon-Ruiz, L., Platret, G., Massieu, E. and Ehrlacher, A., (2005). "The use of thermal analysis in assessing the effect of temperature on a cement paste." *Cement and Concrete Research*, 35(3), 609-613.

Atarashi, D. and Yoshida, N., (2021). "Influence of heating atmosphere on the changes in crystal phase of hardened cement paste." *Cement Science and Concrete Technology*, 75(1), 58-65. (in Japanese)

Baltazar, L., Santana, J., Lopes, B., Paula Rodrigues, M. and Correia, J. R., (2014). "Surface skin protection of concrete with silicate-based impregnations: Influence of the substrate roughness and moisture." *Construction and Building Materials*, 70, 191-200.

Bizzozero, J., Gosselin, C. and Scrivener, K. L., (2014). "Expansion mechanisms in calcium aluminate and sulfoaluminate systems with calcium sulfate." *Cement and Concrete Research*, 56, 190-202.

Daungwilailuk, T., Kitagawa, T., Bui, P. T., Ogawa, Y. and Kawai, K., (2019). "Penetration of moisture, CO_2, and Cl ions in concrete after exposure to high temperature." *Journal of Advanced Concrete Technology*, 17(1), 1-15.

Fares, H., Remond, S., Noumowe, A. and Cousture, A., (2010). "High temperature behaviour of self-consolidating concrete." *Cement and Concrete Research*, 40(3), 488-496.

Gijbels, K., Pontikes, Y., Samyn, P., Schreurs, S. and Schroeyers, W. (2020). "Effect of NaOH content on hydration, mineralogy, porosity and strength in alkali/sulfate-activated binders from ground granulated blast furnace slag and phosphogypsum." *Cement and Concrete Research*, 132, 106054.

Gutberlet, T., Hilbig, R. and Beddoe, R. E., (2015). "Acid attack on hydrated cement - Effect of mineral acids on the degradation process." *Cement and Concrete Research*, 74, 35-43.

Hayashi, D., Sakata, N., Matsuda, Y. and Endo, H., (2019). "Development of silane-and-siloxane-based surface penetrant and demonstration of its long-term durability." *Concrete Journal*, 57(10), 777-784. (in Japanese)

Ishibashi, T., Furuya, T., Hamazaki, N. and Suzuki, H., (2002.). "Investigation of falling on concrete fragments from RC structures." *Doboku Gakkai Ronbunshu*, 711/V-56, 125-134. (in Japanese)

Jia, Z., Chen, C., Shi, J., Zhang, Y., Sun Z. and Zhang P., (2019). "The microstructural change of C-S-H at elevated temperature in Portland cement/GGBFS blended system." *Cement and Concrete Research*, 123, 105773.

Joakim, A., (2015). "*Durability of fire exposed concrete.*" Thesis (PhD). Department of Civil and Architectural Engineering, KTH Royal Institute of Technology, Stockholm.

JSCE, (2005). "*Recommendation for concrete repair and surface protection of concrete structures.*" Tokyo: Japan Society of Civil Engineers. (in Japanese)

Kim, J., Kitagaki, R. and Kido, S., (2016). "Fundamental study on chemical changes in hardened cement using sodium silicate as repair agent." *Proceedings of the Japan Concrete Institute*, 38(1), 1911-1916. (in Japanese)

Kira, K., Makino, Y. and Murata, Y., (1981). "Dehydration and rehydration of ettringite." *Gypsum & Lime*, 170, 7-13. (in Japanese)

Kondo, T., Miyazato, S., Nishino, H. and Yokoi, K., (2019). "A study on Vickers hardness distribution of mortar with silicate type surface penetrants." *Cement Science and Concrete Technology*, 73(1), 333-339. (in Japanese)

Kurokawa, D. and Miyazato, S., (2015). "Proposal of

estimation method for apparent chloride ion diffusion coefficient at reform part by silicate type surface penetrant and trial calculation for corrosion occurrence time." *Journal of Japan Society of Civil Engineers, Ser. E2, (Materials and Concrete Structures)*, 71(2), 124-134. (in Japanese)

Kurumisawa, K., Nawa, T., Owada, H. and Shibata, M., (2013). "Deteriorated hardened cement paste structure analyzed by XPS and ^{29}Si NMR techniques." *Cement and Concrete Research*, 52, 190-195.

Li, Q., Li, Z., Yuan, G. and Shu, Q., (2013). "The effect of a proprietary inorganic coating on compressive strength and carbonation depth of simulated fire-damaged concrete." *Magazine of Concrete Research*, 65(11), 651-659.

Li, Z. and Li, Q., (2011). "Experimental investigation on property recovery of concrete exposed to high temperature." *Journal of Structural and Construction Engineering (Transactions of AIJ)*, 76(666), 1375-1382. (in Japanese)

Liu, X., Feng, P., Yu, X. and Huang, J., (2022). "Decalcification of calcium silicate hydrate (C-S-H) under aggressive solution attack." *Construction and Building Materials (Transactions of AIJ)*, 342(B1), 127988.

Martinez-Ramirez, S. and Palomo, A., (2001a). "Microstructure studies on Portland cement pastes obtained in highly alkaline environments." *Cement and Concrete Research*, 31(11), 1581-1585.

Martinez-Ramirez, S. and Palomo, A., (2001b). "OPC hydration with highly alkaline solutions." *Advances in Cement Research*, 13(3), 123-129.

Masoumi, S., Zare, S., Valipour, H. and Abdolhosseini Qomi, M. J., (2019). "Effective interactions between calcium-silicate-hydrate nanolayers." *The Journal of Physical Chemistry C*, 123(8), 4755-4766.

Maehara, S. and Iyoda, T., (2018). "Study on the effect of rain exposure on carbonation-induced spalling/falling of the cover concrete." *Journal of Japan Society of Civil Engineers, Ser. E2 (Materials and Concrete Structures)*, 74(2), 80-87. (in Japanese)

Midorikawa, T., Takeda, M., Oyamada, T. and Aba, M., (2011). "Properties of chloride ion penetration into concrete with surface penetrants based on long-term exposure test." *Journal of Japan Society of Civil Engineers, Ser. E2 (Materials and Concrete Structures)*, 67(3), 451-461. (in Japanese)

Mota, B., Matschei, T. and Scrivener, K., (2018). "Impact of NaOH and Na$_2$SO$_4$ on the kinetics and microstructural development of white cement hydration." *Cement and Concrete Research*, 108, 172-185.

Pallagi, Á., Tasi, Á., Gácsi, A., Csáti, M., Pálinkó, I., Peintler, G. and Sipos, P., (2012). "The solubility of Ca(OH)$_2$ in extremely concentrated NaOH solutions at 25°C." *Open Chemistry*, 10(2), 332-337.

Réus, G. C. and Medeiros, M. H. F., (2020). "Chemical realkalization for carbonated concrete treatment: Alkaline solutions and application methods." *Construction and Building Materials*, 262(30), 120880.

Someya, N. and Kato, Y., (2014). "Fundamental study on modification effect and penetration mechanism of silicate-based surface penetrants." *Concrete Research and Technology*, 25, 181-189. (in Japanese)

Sugiyama, D., (2008). "Chemical alteration of calcium silicate hydrate (C-S-H) in sodium chloride solution." *Cement and Concrete Research*, 38(11), 1270-1275.

Takeda, N., Era, K., Hamasaki, H., Yamaguchi, T. and Tanaka, H., (2021). "Preventive maintenance of concrete structures, current status and suggestions." *Concrete Journal*, 59(10), 857-864. (in Japanese)

Tran, P. C., Kobayashi, K., Asano, T. and Kojima, S., (2018). "Carbonation proofing mechanism of silicate-based surface impregnations." *Journal of Advanced Concrete Technology*, 16(10), 512-521.

Trapote-Barreira, A., Porcar, L., Cama, J., Soler, J. M. and Allen, A. J., (2015). "Structural changes in C-S-H gel during dissolution: Small-angle neutron scattering and Si-NMR characterization." *Cement and Concrete Research*, 72, 76-89.

Walker, C. S., Sutou, S., Oda, C., Mihara, M. and Honda, A., (2016). "Calcium silicate hydrate (C-S-H) gel solubility data and a discrete solid phase model at 25°C based on two binary non-ideal solid solutions." *Cement and Concrete Research*, 79, 1-30.

Xu, L., Wang, J., Li, K., Hao, T., Li, Z., Li, L., Ran, B. and Du, H., (2023). "New insights on dehydration at elevated temperature and rehydration of GGBS blended cement." *Cement and Concrete Composites*, 139, 105068.

Yan, Y., Yang, S. Y., Miron, G. D., Collings, I. E., L'Hôpital, E., Skibsted, J. and Lothenbach, B., (2022). "Effect of alkali hydroxide on calcium silicate hydrate (C-S-H)." *Cement and Concrete Research*, 151, 106636.

Zhang, Q., Ye, G. and Koenders, E., (2013). "Investigation of the structure of heated Portland cement paste by using various techniques." *Construction and Building Materials*, 38, 1040-1050.